



## Instrumentation Readings versus Numerical Analysis of Taham Dam

M. Javanmard<sup>\*a</sup>, F. Amiri<sup>a</sup>, S. M. Safavi<sup>b</sup><sup>a</sup> Department of Civil Engineering, University of Zanjan, Zanjan, Iran<sup>b</sup> Department of Civil Engineering, Zanjan Branch, Islamic Azad University, Zanjan, Iran

## P A P E R I N F O

## Paper history:

Received 24 August 2018

Received in revised form 18 December 2018

Accepted 03 January 2019

## Keywords:

Taham Dam

Stress

Pore Water Pressure

Numerical Analysis

Instrumentation

## A B S T R A C T

Dam construction is one of the challenges among large-scale projects of a country. Among different types of dams, due to special features, earth dams are the most kind of dams that were constructed in Iran in the past three decades. Features such as efficiency and stability of earth dams have an important effect on their operation and prevent them to be damaged. Taham dam is clay core dam which is constructed in Zanjan province in Iran. After dam impoundment, the stresses and distribution of pore water pressure of the Taham earth dam were investigated and measured by using the instrumentation installed in dam body. Measured values then compared with the obtained results by numerical analysis of the Dam. For numerical analysis PLAXIS code has been used. This comparison showed that the pore water pressures in the dam is similar with the results of numerical analysis, but the stresses in the dam are lower than results of numerical analysis in most areas of dam.

doi: 10.5829/ije.2019.32.01a.04

## NOMENCLATURE

$\varepsilon$	Strain	$\sigma$	Total stress
$\underline{\varepsilon}^e$	Elastic strain matrix	$\sigma'$	Effective stress
$\underline{\varepsilon}^p$	Plastic strain matrix	$\dot{\sigma}'$	Effective stress rate
$\dot{\varepsilon}$	Strain rate	$E$	Young's module
$\underline{\dot{\varepsilon}}^e$	Elastic strain rate matrix	$E'$	Effective Young's module
$\underline{\dot{\varepsilon}}^p$	Plastic strain rate matrix	$\nu$	Poisson's ratio
$\gamma$	Shear strain	$\nu'$	Effective Poisson's ratio
$\dot{\gamma}$	Shear strain rate	$\underline{D}^e$	Elastic material stiffness matrix

## 1. INTRODUCTION

Generally, dams are used as one of the main sources of reservoirs. Therefore, they have special significance and their design must be done carefully. Because of their construction cost is enormous and damage to them is normally a catastrophe, and results in loss of lives, massive and wide spread damage to structures [1].

Therefore, the risk of dam failure should be as low as possible. Also monitoring of dams operation and their maintenance procedure should be done continuously during their life time. This matter is carried out normally in three main phases, which are during their construction, first impoundment and during their operation. Correct monitoring requires having accurate knowledge of dam behavior. This could be achieved by meticulous measurements of desired variables which is so called dam instrumentations. Dam instrumentations should be done in a way that dam operator be aware of

\*Corresponding Author Email: mehranj@znu.ac.ir (M. Javanmard)

how they behave in different situations and time periods [2]. By analyzing the instrumentations readings, dam behavior could be predicted, and in the case of occurrence of serious problems in the dam body, preventative actions could be done. Generally, materials for construction of dams are clay core and rock-fill materials, so they may be referred to as fill-type dams or embankment dams [3]. Dam construction is always a challenge for engineers, and building them is one of the most confrontation issues in civil engineering projects. Research has been done for their behavior under applied loads, and seepage through their body. Marandi et al. [4], investigated the effects of location of drainage blanket on earth dam settlement. They found that in a 3-d model this effect is more than that of in 2-D model. Dynamic behavior of a rockfill dam built in Fars province in Iran was studied by Noorzai and Mohammadian [4]. In their research, obtained results showed that the dam could resist the design basis level of earthquake record.

In the past, due to lack of technical knowledge, the height of earth dams was limited. But, with advances in advent of new techniques and codes, and better understanding of soil characteristics and its behavior, construction of clay dams with a high elevation and big reservoir is possible, for example, earth dams with a height more than 300 meters are built in recent years [6].

Generally, maintenance procedure for dams compared to that of other engineering structures is more crucial and require more attention. Due to the high cost of dams construction and severe damage caused by their failure, controlling the stability of the dam during construction and after that, is very important. Therefore, the dam behavior should be analyzed during construction and after that. Monitoring the behavior of clay dam, and rock-fill dam could be done by measuring of total stress, pore water pressure, or its displacement.

## 2. MAIN FEATURE OF TAHAM DAM

Taham dam is an earth dam with clay core and is located in 15 kilometers North West of Zanzan City and at 8 kilometers away from Taham village (see Figure 1). The dam is about 300 meters downstream of the intersection of Taham River and the Gale River. The height of Taham dam is 123.7 m, the length of the crest is 451 m and the volume of the water reservoir is approximately  $85 \times 10^6 m^3$  [5]. Figure 1 shows an aerial photo of Taham dam.

The instrumentation of dam in order to monitor its behavior was chosen based on the profile of dam body and its geological status is shown in Figures 2, and 3.



Figure 1. Location of Taham dam



Figure 2. Installation of Instrumentations

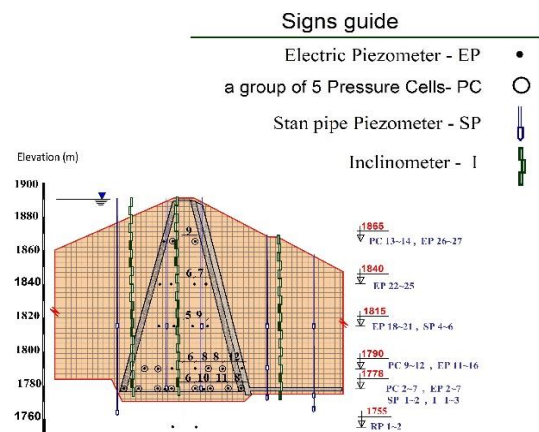


Figure 3. Location of instrumentations

The position of the devices used in the dam is adjusted and calibrated so that their readings can be easily done. The purpose of such a instrumentation is to measure and monitor the pore water pressure in the foundation and body of the dam, internal stresses, internal and external displacement of the dam [8].

Usually earth pressure cells are installed in five direction (Figure 4). These Directions are vertical while parallel to dam axis (Figure 4-a), 45-degree to upstream (Figure 4-b), horizontal (Figure 4-c), 45-degree to downstream (Figure 4-d) and vertical while normal to dam axis (Figure 4-e).

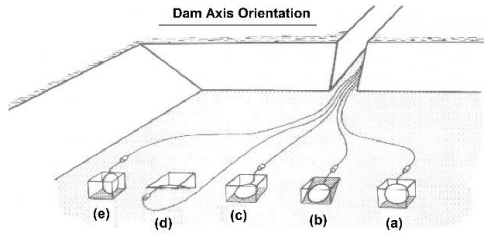


Figure 4. Cell pressure orientation in the dams [6]

Figure 5 shows the location and orientation of Pressure Cells (PC) and Electrical Piezometers (EP) at 1781 m elevation. In Taham dam pressure cells installed horizontally are called (PC-X-3) and measured vertical stresses.

### 3. NUMERICAL ANALYSIS

To find a closed form solution for a geotechnical problem is usually difficult, if not impossible. Therefore, numerical analysis normally are being used to encountered problems in the field of geotechnics. However, to do so, a powerful code and a profound understanding of related theory, such as finite element method, to interpret the obtained results are essentials [7]. Toufigh [8], has studied the effect of external loads and variation of total head on consolidation settlement. In this research Least Square Finite Element formulation has been used. Eight nodal elements also were used to model a few seepage problems. Fakhimi, and Moosavi [9], have used numerical study in order to study the permanent displacement of slopes. They found that in a granular soil media, there is a better agreement between numerical results and theoretical analysis than that of cohesive soil. In this study, the Plaxis code was used for numerical analysis of Taham dam and obtained results were compared to measured ones. Plaxis code was developed for analysis of deformation and stability of dams, water flow analysis in dams, embankments, sheet piles, etc. Both linear and nonlinear behavior for soil and rock media could be used in models. This software can model different loading conditions and boundary conditions by 6-node or 15-

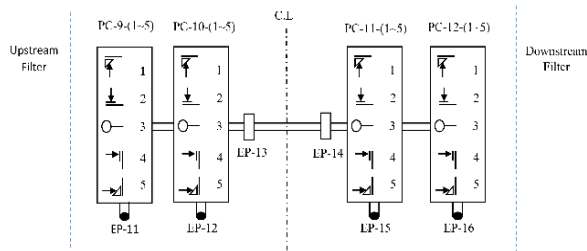


Figure 5. Arrangement of instrumentations at elevation 1790 m

node elements. Various criteria such as hardening-soil, Mohr-Coulomb, soft soil creep, could be used in this program for soil media.

### 4. MATERIALS AND METHODS

In this research Mohr-Coulomb criteria has been used for to model the behavior of soil media. In elastoplastic behavior, strain and strain rate are divided into elastic and plastic parts, Equations (1), and (2):

$$\underline{\varepsilon} = \underline{\varepsilon}^e + \underline{\varepsilon}^p \quad (1)$$

$$\underline{\dot{\varepsilon}} = \underline{\dot{\varepsilon}}^e + \underline{\dot{\varepsilon}}^p \quad (2)$$

Elastic stress-strain relationship is based on Hook's law, which is shown in Equation (3).

$$\begin{bmatrix} \dot{\sigma}'_{xx} \\ \dot{\sigma}'_{yy} \\ \dot{\sigma}'_{zz} \\ \dot{\sigma}'_{xy} \\ \dot{\sigma}'_{yz} \\ \dot{\sigma}'_{zx} \end{bmatrix} = \frac{E'}{(1-2\nu')(1+\nu')} \begin{bmatrix} 1-\nu' & \nu' & \nu' & 0 & 0 & 0 \\ \nu' & 1-\nu' & \nu' & 0 & 0 & 0 \\ \nu' & \nu' & 1-\nu' & 0 & 0 & 0 \\ 0 & 0 & 0 & 0.5-\nu' & 0 & 0 \\ 0 & 0 & 0 & 0 & 0.5-\nu' & 0 \\ 0 & 0 & 0 & 0 & 0 & 0.5-\nu' \end{bmatrix} \begin{bmatrix} \dot{\varepsilon}_{xx} \\ \dot{\varepsilon}_{yy} \\ \dot{\varepsilon}_{zz} \\ \dot{\gamma}_{xy} \\ \dot{\gamma}_{yz} \\ \dot{\gamma}_{zx} \end{bmatrix} \quad (3)$$

Substitution of Equation (2) into Equation (3) leads to Equation (4).

$$\underline{\sigma}' = \underline{D}^e \underline{\dot{\varepsilon}}^e = \underline{D}^e (\underline{\dot{\varepsilon}} - \underline{\dot{\varepsilon}}^p) \quad (4)$$

According to the theory of plasticity the plastic strain rates can be represented as vectors perpendicular to the yield surface. Plasticity involves the development of irreversible strains. A yield function, "f", is introduced as a function of stress and strain to assess whether or not plasticity occurs. The plastic yielding is related with the f=0 condition. These conditions can be presented as a surface in principal stress space. A perfectly-plastic model is a constitutive model with a fixed yield surface, i.e. a yield surface that is fully defined by model parameters. Also, the model is not affected by (plastic) straining. For stress states represented by points within the yield surface, the behaviour is purely elastic and all strains are reversible. For Mohr-Coulomb type yield functions, the theory of associated plasticity overestimates dilatancy. Therefore, in addition to the yield function, a plastic potential function g is introduced. The case  $g \neq f$  is denoted as non-associated plasticity. In general, the plastic strain rates are written as:

$$\underline{\dot{\varepsilon}}^p = \lambda \frac{\partial g}{\partial \underline{\sigma}'} \quad (5)$$

in which  $\lambda$  is the plastic multiplier. For purely elastic behaviour  $\lambda$  is zero, whereas in the case of plastic behaviour  $\lambda$  is positive [10].

$$\lambda = 0 \text{ for: } f < 0 \text{ or: } \frac{\partial f^T}{\partial \underline{\sigma}'} D^e \underline{\dot{\epsilon}} \leq 0 \quad (\text{Elasticity}) \quad (6a)$$

$$\lambda > 0 \text{ for: } f < 0 \text{ or: } \frac{\partial f^T}{\partial \underline{\sigma}'} D^e \underline{\dot{\epsilon}} \leq 0 \quad (\text{Plasticity}) \quad (6b)$$

The relationship between the effective stress rates and strain rates for elastic perfectly-plastic behaviour [11]:

$$\dot{\underline{\sigma}}' = (D^e - \frac{\alpha}{d} D^e \frac{\partial g}{\partial \underline{\sigma}'} \frac{\partial f^T}{\partial \underline{\sigma}'} D^e) \underline{\dot{\epsilon}} \quad (7)$$

where  $d = \frac{\partial g}{\partial \underline{\sigma}'} D^e \frac{\partial f^T}{\partial \underline{\sigma}'}$  For elastic behaviour the parameter  $\alpha$  is zero and for plastic behaviour is equal to unity [10]. The standard form of Mohr-Coulomb yield shape surface may be shown as in Equation (8) [12]:

$$f_{(i,j,k)} = \frac{1}{2} [|\sigma'_{(j,k,i)} - \sigma'_{(k,i,j)}| + \frac{1}{2} [|\sigma'_{(j,k,i)} + \sigma'_{(k,i,j)}| \sin \phi - c \cos \phi] \leq 0 \quad (8)$$

In Equation (8), “ $c$ ” and “ $\phi$ ”, are cohesion and friction angle, respectively.

### 5. SOIL PROPERTIES

Soil properties used in numerical analysis of Taham dam, are presented in Table 1. The properties of gravel and sand, clay, and bedrock have been used in modeling of shells, core and foundation, respectively. These properties were obtained from laboratory test on Taham dam materials.

Dam section at its highest elevation (i.e. at 1891 m altitude) has been selected for analysis. In addition to the body of dam, a part of foundation (180 meters in depth) was also included in the model. The model of considered for numerical analysis has a height of 123 m, with a side slope of 1 in 2 on upstream side and 1 in 1.8 on downstream side, with a 180 m foundation. The reservoir level was 118 m high along with 10 m underneath the ground, for representing the groundwater. Suitable hydraulic boundary conditions were assigned. Closed flow boundaries were assigned to left, right and bottom of foundation. Equipotential lines were specified at the upstream and downstream sides.

Figure 6 shows the earth dam modeled section. The accuracy of the calculations is associated with the mesh size, therefore the mesh sizes assigned to core, shell and foundation were selected to be very fine, fine and medium respectively. Finite element mesh for the model is shown in Figure 7. Obtained mean stresses, effective stresses, and effective mean stresses from the numerical analysis are presented in Figures 8, 9, and 10, respectively. Furthermore, Figure 11 shows the pore water pressure.

TABLE 1. Soil Properties

Parameter	Clay	Gravel and sand	Bedrock
Type of behavior	Undrained	Drained	Drained
$\gamma$ (kN/m <sup>3</sup> )	16.9	20.02	25
$\gamma'$ (kN/m <sup>3</sup> )	20.8	23.10	26
$k_x$ (m/day)	1.768e-3	1.83	0.035
$k_y$ (m/day)	10768e-3	1.83	0.035
E (MPa)	1.001 e-4	7.92e4	8.7e6
$\nu$	0.258	0.268	0.28
$c$ (kN/m <sup>2</sup> )	66	5.4	251
$\phi$ (°)	28.4	38.4	47
$\psi$ (°)	0	5.6	8

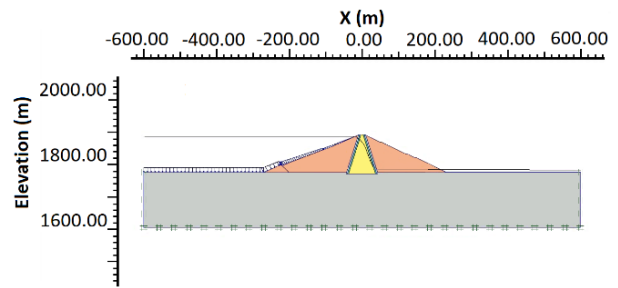


Figure 6. Dam model for numerical analysis

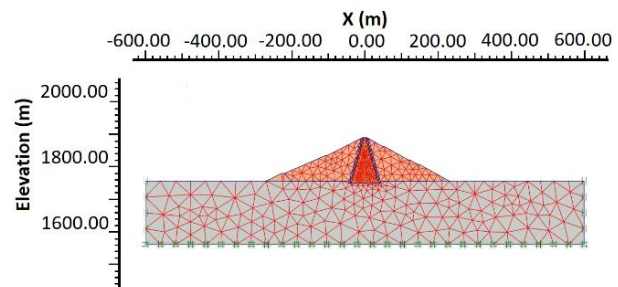


Figure 7. Generated mesh for the model

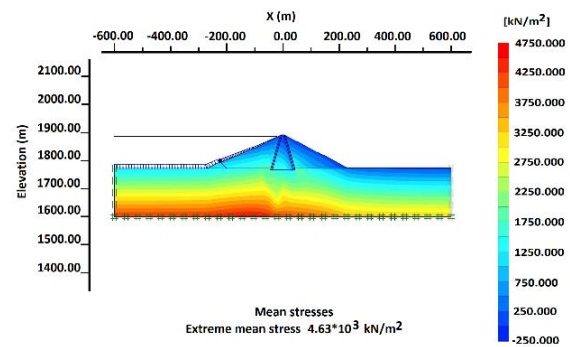


Figure 8. Mean stresses

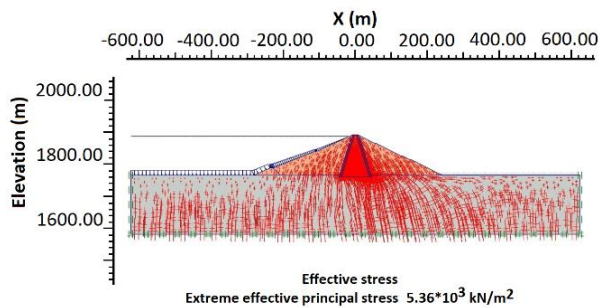


Figure 9. Effective stresses

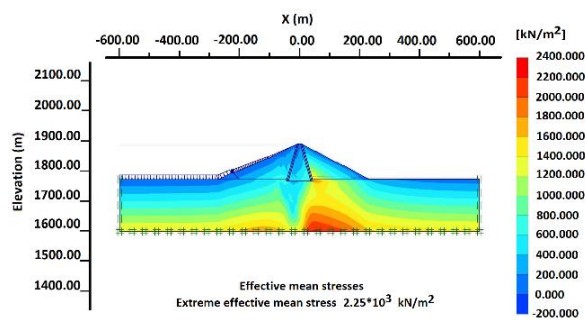


Figure 10. Effective mean stresses

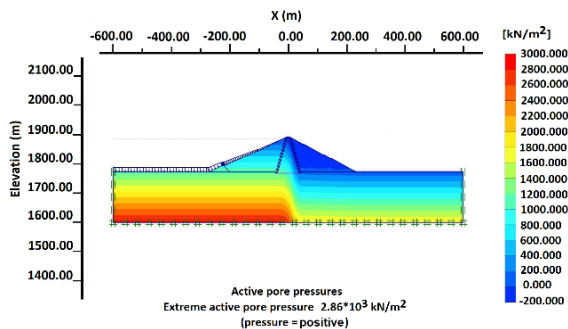


Figure 11. Pore water pressures

## 7. COMPARISON OF MONITORED FIELD DATA, AND CALCULATED NUMERICAL ANALYSIS ONES

Table 2, shows calculated stresses by carrying out numerical analysis, and those measured by installed pressure cells in the body of dam. Vertical stresses results in the model are also shown graphically at 1778 m and 1790 m, elevation in Figures 12, and 13, respectively, versus vertical stresses obtained from the pressure cells that are installed horizontally (PC-X-3). Table 3, and Figures 14, 15, 16, 17, and 18 show calculated pore water pressure compared with the piezometric head obtained from electrical piezometers (EP) reading.

TABLE 2. Numerical analysis vs. field data for pressure cells

Code of device	Installation location		Instrumentation Reading (kPa)	Numerical analysis (kPa)
	x (m)	y (m)		
PC - 2-1	-29	1778	Damaged	-
PC - 2-2	-29	1778	Damaged	1310
PC - 2-3	-29	1778	483.95	1331
PC - 2-4	-29	1778	1176	1830
PC - 2-5	-29	1778	889.08	-
PC - 3-1	-18	1778	928.05	-
PC - 3-2	-18	1778	Damaged	1306
PC - 3-3	-18	1778	Damaged	1303
PC - 3-4	-18	1778	1272.9	1782
PC - 3-5	-18	1778	1072.3	-
PC - 4-1	-7	1778	664.82	-
PC - 4-2	-7	1778	1008.6	1288
PC - 4-3	-7	1778	1561.1	1259
PC - 4-4	-7	1778	951.11	1762
PC - 4-5	-7	1778	626.63	-
PC - 5-1	7	1778	621.5	-
PC - 5-2	7	1778	904.18	1166
PC - 5-3	7	1778	1409.1	1098
PC - 5-4	7	1778	1035.6	1596
PC - 5-5	7	1778	550.63	-
PC - 6-1	18	1778	586.84	-
PC - 6-2	18	1778	706.47	1033
PC - 6-3	18	1778	1426.4	783
PC - 6-4	18	1778	1893.1	1204
PC - 6-5	18	1778	75.07	-
PC - 7-1	29	1778	132.94	-
PC - 7-2	29	1778	754.09	962
PC - 7-3	29	1778	993.53	556
PC - 7-4	29	1778	631.78	815
PC - 7-5	29	1778	437.32	-
PC - 9-1	-25	1790	Damaged	-
PC - 9-2	-25	1790	1018.5	1090
PC - 9-3	-25	1790	1279.6	1144
PC - 9-4	-25	1790	Damaged	1544
PC - 9-5	-25	1790	876.64	-
PC - 10-1	-16	1790	890.55	-
PC - 10-2	-16	1790	811.9	1061
PC - 10-3	-16	1790	726.27	1107
PC - 10-4	-16	1790	563.97	1501

PC -10-5	-16	1790	572.73	-
PC -11-1	16	1790	424.21	-
PC -11-2	16	1790	Damaged	1004
PC -11-3	16	1790	800.32	704
PC -11-4	16	1790	324.05	1023
PC -11-5	16	1790	264.94	-
PC -12-1	25	1790	392.76	-
PC -12-2	25	1790	480.22	898
PC -12-3	25	1790	678.2	505
PC -12-4	25	1790	172.88	706
PC -12-5	25	1790	240.09	-
PC -13-1	-7	1865	Damaged	370
PC -13-2	-7	1865	219.68	219
PC -13-3	-7	1865	218.94	-
PC -13-4	-7	1865	235.11	-
PC -13-5	-7	1865	Damaged	205
PC -14-1	7	1865	107.03	358
PC -14-2	7	1865	97.78	161
PC -14-3	7	1865	94.06	-
PC -14-4	7	1865	132.75	-
PC -14-5	7	1865	Damaged	134

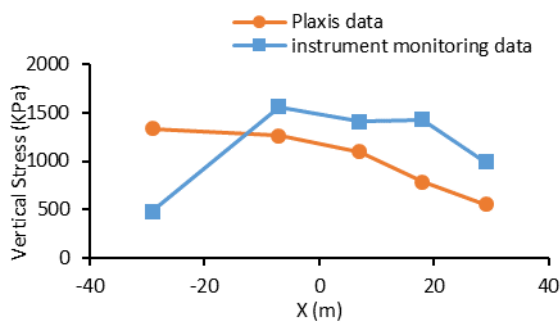


Figure 12. Numerical analysis results vs. pressure cell readings at elevation of 1778 m

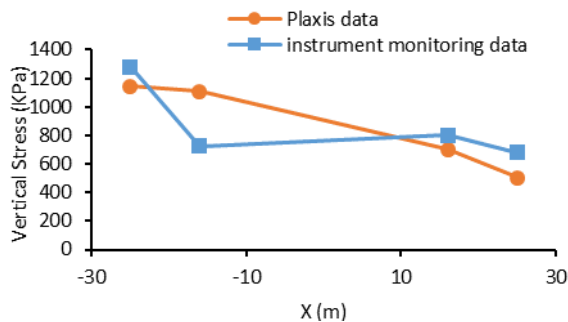


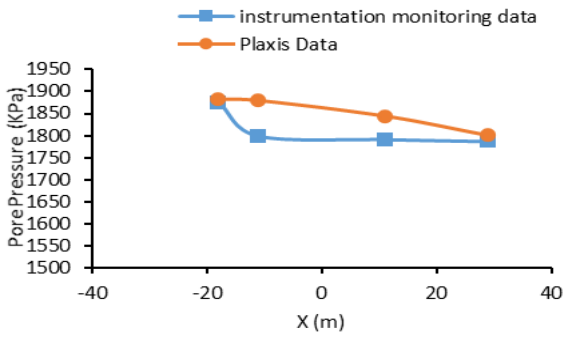
Figure 13. Numerical analysis results vs. pressure cell readings data at elevation of 1790 m

As it is seen in the tables and figures, electrical piezometer reading are almost consistent with the obtained results of numerical analysis. A few discrepancies at some locations may be related to the malfunction of EPs. In regard to the pressure cells' reading, in some locations, there is a considerable inconsistency between instrumentation's reading and the numerical analysis results. This mismatch could be related to the following reasons:

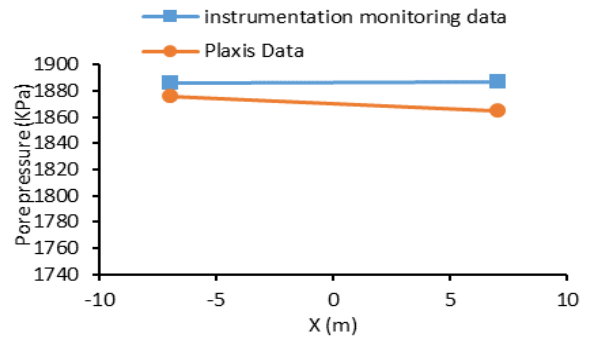
1. Mohr-Coulomb criteria considered for the soil media, may not be an exact model to represent its behavior. In addition to that, allocated soil properties are not 100% , the same as they are in the field. To these, error of computation which is normal in most codes, could be added.
2. Existence of material heterogeneity in different layers of soil media.
3. Malfunction of instrumentation installed in the dam.

TABLE 3. The numerical result for pore water pressure vs. electrical piezometers reading

Code of device	Installation location		Instrumentation reading (KPa)	Numerical analysis (KPa)
	x (m)	y (m)		
EP - 2	-29	1778	Damaged	1886
EP - 3	-18	1778	1876.17	1883
EP - 3-1	-11	1778	1799.53	1880
EP - 4	-7	1778	Damaged	1875
EP - 5	7	1778	Damaged	1858
EP - 5-1	11	1778	1791.72	1844
EP - 6	18	1778	Damaged	1821
EP - 7	29	1778	1787.32	1799
EP - 11	-25	1790	1875.38	1886
EP - 12	-16	1790	1878.94	1883
EP - 13	-7	1790	1870.86	1876
EP - 14	7	1790	1846.05	1858
EP - 15	16	1790	1824.49	1827
EP - 16	25	1790	1799.14	1804
EP - 18	-16	1815	1870.6	1882
EP - 19	-6	1815	Damaged	1875
EP - 20	6	1815	1870.55	1859
EP - 21	15	1815	1833.39	1823
EP - 22	-15	1840	1883.57	1882
EP - 23	-7	1840	1869.98	1876
EP - 24	7	1840	1853.3	1857
EP - 25	15	1840	1848.61	1841
EP - 26	7	1865	1887.17	1865
EP - 27	-7	1865	1886.38	1876



**Figure 14.** Numerical analysis vs. electrical piezometers readings (installed in 1778 m level)



**Figure 18.** Numerical analysis vs. electrical piezometers readings (installed in 1865 m level)

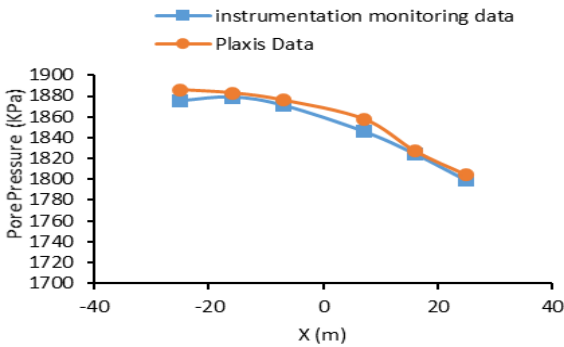


**Figure 15.** Numerical analysis vs. electrical piezometers readings (installed in 1790 m level)

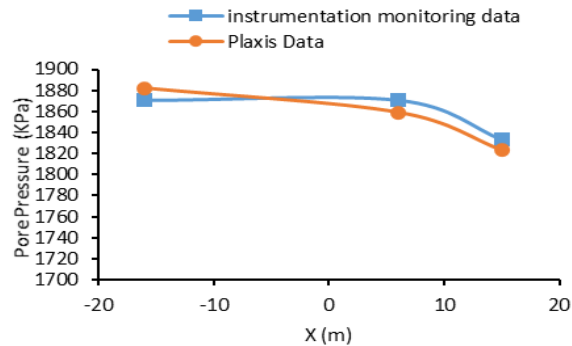


**Figure 16.** Numerical analysis vs. electrical piezometers readings (installed in 1815 m level)

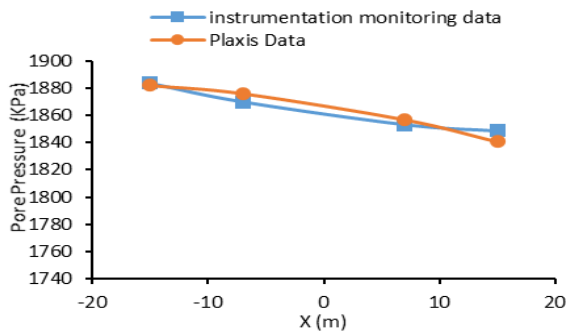


**Figure 17.** Numerical analysis vs. electrical piezometers readings (installed in 1840 m level)

Also, in the clay core of the earth dam, at a section with higher altitude, pore water pressure is less than that of section at lower altitude. However, in the clay core region which is closer to the reservoir, pore water pressure increases. It should be noted that since for numerical analysis, degree of saturation always consider to be 100% in the Plaxis code, the instrumentation readings and calculated numerical analysis in the regions of the core that are closer to the reservoir had a better match. Finally for the instrumentation installed at a higher level, differences in instrumentation reading and calculated numerical analysis ones are more visible.

Based on Table 3, water pressure at each defined level decreases from the upstream to downstream, which indicates the proper functioning of the clay core. As expected, the highest vertical stress is at elevation of 1778 m. The trend of pressure changes shows acceptable values.

### 7. CONCLUSIONS

Based on the obtained data either from field reading, or numerical analysis, following conclusions may be drawn:

1. Comparison of pore water pressure from the instrumentations' reading installed in dam's core at different levels and the results of the numerical analysis shows that the value of pore water pressure for both methods, near the reservoir is better than that of regions away from the reservoir. The reason for this is the PLAXIS shortcoming in calculating of water pressure in the semi-saturated soils. The program considers the saturation percentage of the material to be 100%, which results in higher water pressure.
2. Considering vertical pressure, the results of instrumentations' readings were lower than that of numerical analysis and the difference between these two were about 28%.
3. The results obtained from Plaxis were compatible

with the results of electrical piezometers and the difference between these two were less than 1%.

## 8. REFERENCES

- Baecher, G. B., Paté, M. E. and De Neufville, R., "Risk of dam failure in benefit-cost analysis", *Water Resources Research*, Vol. 16, No. 3, (1980), 449-456.
- Verma, D., Setia, B. and Arora, V., "Experimental study of breaching of an earthen dam using a fuse plug model", *International Journal of Engineering*, Transactions A: Basics, Vol. 30, No. 4, (2017), 479-485.
- Athani, S. S., Solanki, C. and Dodagoudar, G., "Seepage and stability analyses of earth dam using finite element method", *Aquatic Procedia*, Vol. 4, No., (2015), 876-883.
- Marandi, S.M., Safapour, P., Movahed Asl, R. and Bagheripour, M. H., "Earthquake Induced Permanent Displacement of Slopes: A Numerical Study", *International Journal of Engineering*, Vol. 18, No. 2, (2005), 187-195.
- Noorzadei, J., Mohammadian, E., "Seismic Respose of the Kavar Concrete Face Rockfill Dam", *International Journal of Engineering Transaction B: Applications*, Vol. 15, No.4, (2002), 333-346.
- Saeedinia, A., Akbari, H., Salemi, I., "Earth Dam's precise instruments", Sepa Sad Engineering Co. publication, (2012).
- Rashidi, M., Haeri, S. M., "Evaluation of behaviors of earth and rockfill dams during construction and initial impounding using instrumentation data and numerical modeling", *Journal of Rock Mechanics and Geotechnical Engineering*, Vol. 9, No. 4, (2017), 709-725.
- Mellisakhteman Co., "Report of Installed Tools at Taham Dam", (2005).
- Shoghli, A., Mirghasemi, A. A., Lim, Y., "Assessing and Evaluating the Operation of Pressure Cells in Embankment Dams: A Case Study of Five Iranian Embankment Dams", 36th Annual United States Society on Dams conference, Denver, Colorado, April 11-15, (2016).
- Vahdati, P., "Identification of soil parameters in an embankment dam by mathematical optimization", PhD diss., Luleå Tekniska Universitet, (2014).
- Toufigh, M. M., "Seepage with Nonlinear Permeability by Least Square FEM", *International Journal of Engineering Transaction B, Applications*, Vol. 15, No. 2, (2002), 125-134.
- Fakhimi, A. A., Moosavi, M. J., "Earthquake Induced Permanent Displacement of Slopes, A Numerical Study", *International Journal of Engineering*, Vol. 13, No. 4, (2000), 73-80.
- Brinkgreve, R. B. J., Kumarswamy, S., Swolfs, W.M. and Foria, F., "Plaxis 2D material models manual", Plaxis bv, (2018).
- Vermeer, P.A. and De Borst, R., "Non-associated plasticity for soils, concrete and rock", *Heron*, Vol. 29, No. 4, (1984).
- Mollaie, R., Mollaie, M., Gheidari, M. H. N., Elahi, H. A., "Evaluation of Gelabar earth dam behavior during construction and first watering by the method of limited components and comparison with real amount resulted by precise instruments data", *European Online Journal of Natural and Social Sciences*, Vol. 3, No. 4, (2014), 657-676.

## Instrumentation Readings versus Numerical Analysis of Taham Dam

M. Javanmard<sup>a</sup>, F. Amiri<sup>a</sup>, S. M. Safavi<sup>b</sup>

<sup>a</sup> Department of Civil Engineering, University of Zanjan, Zanjan, Iran

<sup>b</sup> Department of Civil Engineering, Zanjan Branch, Islamic Azad University, Zanjan, Iran

### P A P E R I N F O

چکیده

#### Paper history:

Received 24 August 2018

Received in revised form 18 December 2018

Accepted 03 January 2019

#### Keywords:

Taham Dam

Stress

Pore Water Pressure

Numerical Analysis

Instrumentation

یکی از چالش‌ها در بین پروژه‌های بزرگ مقیاس توسعه‌ای یک کشور، ساخت سد است. در بین انواع گوناگون سدها، بدلیل خصوصیات خاص سدهای خاکی، آن‌ها بیشترین نوع سد ساخته شده در ایران در سه دهه گذشته هستند. خصوصیات نظیر بهره‌وری و پایداری سدهای خاکی اثر مهمی روی کارکردشان داشته و مانع بروز خسارت به آنها می‌شود. سد ته‌م، سدی خاکی می‌باشد که در استان زنجان ایران ساخته شده است. پس از آبیگری سد، تنش‌ها و توزیع فشار آب حفره‌ای در سد ته‌م بررسی و با استفاده از ابزار دقیق نصب شده در سد اندازه‌گیری شدند. این مقادیر اندازه‌گیری شده سپس با نتایج بدست آمده از تحلیل عددی سد مقایسه شدند. برای تحلیل عددی برنامه "پلکسیس" مورد استفاده قرار گرفت. این مقایسه نشان داد که فشار آب حفره‌ای مشابه نتایج تحلیل عددی بوده ولی تنش‌های در سد کمتر از نتایج تحلیل عددی در اکثر قسمت‌های سد است.

doi: 10.5829/ije.2019.32.01a.04